LA-UR-13-28618
Approved for public release; distribution is unlimited.

Title: Elastic precursor decay in S-200F Beryllium

Author(s): Adams, Chris D.
Anderson, William W.
Gray, George T. III
Blumenthal, William R.

Intended for: APS-SCCM & AIRAPT-24 Joint Conference Proceedings

Issued: 2013-11-08

Elastic precursor decay in S-200F beryllium

Chris D Adams, William W Anderson, William R Blumenthal and George (Rusty) T Gray III

Los Alamos National Laboratory, Los Alamos, NM, USA

E-mail: cadams@lanl.gov

Abstract. We have performed a series of plate impact experiments on vacuum hot-pressed (VHP) S-200F Be at peak shock stresses between 2.1 and 23.0 GPa to gain insight into the dynamic strength (Hugoniot elastic limit (HEL)), equation-of-state, and damage behavior of this technologically important material. In this paper we focus on our VISAR observations of the evolution of elastic precursor amplitude with Be target thickness in a series of plate impact experiments conducted in both transmission and reverse geometry. We observe monotonic decay in precursor amplitude with run distance for sample thicknesses between 4 and 8 mm and present the HEL values obtained from these experiments. We will discuss the observed precursor decay with respect to the relative roles of twinning and dislocation-mediated slip in the overall dynamic material mechanical response.

1. Introduction

Due to its high strength-to-weight ratio, there are many potential applications for Be in aerospace and defense. In addition to its strength-to-weight attributes, the dynamic mechanical response of Be across a range of strain rates is also a consideration in its selection for any particular application where dynamic loads are involved. Due to the toxicity of Be, the volume of experimental work considering the dynamic behavior of Be is limited. We have taken advantage of an existing capability used primarily to study the dynamic behavior of other hazardous materials to investigate the dynamic response of Be through plate impact experiments.

The data presented here represents a small part of a broader ongoing effort to better understand the dynamic strength, damage, and equation-of-state (EOS) behavior of Be. We focus in this presentation on the dynamic strength behavior of vacuum hot-pressed (VHP) S-200F Be. In particular we present our observations of the evolution of the elastic wave amplitude with run distance (target thickness) derived from a series of plate impact experiments. Of the various grades of Be available, the VHP S-200F Be grade is characterized by a lower BeO content and finer grain size than the preceding S200-D or -E grades.[1] The vast majority of earlier investigations of the dynamic behavior of S200 Be were conducted on S200-D, or -E, grades.

2. Experimental

A series of plate impact experiments were conducted in either a transmission (Be target) or reverse (Be impactor) geometry on the 40-mm Impact Test Facility at Los Alamos National Laboratory. The configurations of the experiments considered here are presented in Table 1. For experiments conducted in transmission geometry, S200-F Be targets were impacted

with either another S200-F Be sample, Z-cut Quartz, Z-cut Sapphire, annealed OFHC Cu, or annealed Ta depending on the desired peak state stress. A single reverse geometry experiment (55-476) was conducted in which an S-200F Be impactor placed in the projectile was made to impact a Z-cut Sapphire window serving as a target and analyzer window. In either geometry, VISAR was employed as the principal diagnostic to observe wave profile evolution at either the impact surface in the case of reverse geometry or the rear surface of the target after shock wave propagation through the target in the case of transmission geometry. Lead zirconate titanate (PZT) piezo-electric impact pins distributed around the periphery of the target were used to determine impact time, relative target/impactor tilt at time of impact, and trigger the VISAR. Radial shorting pins were used to determine impact velocity.

Table 1. Summary of experimental configurations and calculated stresses for the elastic and final (plastic) shock states. HEL values presented in parenthesis for shots 55-429 and 55-466 were calculated using the longitudinal wave speeds (c_L) measured pre-shot. All others were calculated using timing from the experiment.

Exp.	Impactor/Target Configuration	Be Thickness (mm)	Impact Velocity (mm/μs)	Peak Stress (GPa)	HEL (GPa)
55-429	Be/Be	3.9850	0.721	5.63	0.139(0.145)
55-430-P30	Be/Be	3.9670	1.246	10.1	0.153
55-432	Z-Sapphire/Be	5.9630	0.654	7.63	0.104
55-433-P32	Ta/Be	3.9875	1.419	19.0	0.147
55-436	Z-Quartz/Be	3.9820	0.255	2.09	0.133
55-444	Z-Quartz/Be	5.9563	0.409	3.37	0.113
55-450-P38	Ta/Be	7.9230	1.155	15.1	0.086
55-454	Z-Quartz/Be	8.0715	0.263	2.12	0.089
55-466	Cu/Be	4.9920	0.522	5.76	0.138(0.145)
55-476	Be/Z-Sapphire	1.9563	0.661	7.87	——

All samples were machined from a single billet of VHP S200-F Be. Longitudinal c_L and shear c_s wave speeds were measured using a pulse-echo technique on each sample prior to the experiments. Initial densities (ρ_0) were determined using immersion techniques. The measured, pre-shot, wave speeds were within 1% of those reported for Be.[2] Details of the sample preparation are discussed in [3].

3. Results and Discussion

Table 1 presents the calculated peak stress levels achieved by the elastic precursor (HEL) and plastic waves in the Be target material following shock loading in transmission geometry. The stress levels were determined using standard methods of impedance matching along with impact times determined by PZT pins, and wave arrival times from VISAR. The values for the HEL for the 4 experiments listed at the top of the table are the same as those presented earlier [3] with the exception of the HEL derived from experiment 55-433-P32. The HEL determined for this experiment has been re-calculated based on a better estimate of the precursor amplitude derived from the original VISAR data resulting in a 13% decrease in the reported value. Also note, we are not able to overdrive the elastic precursor in any of the experiments conducted to date having final state stress levels up to 23.0 GPa; validation of the high strength of Be.

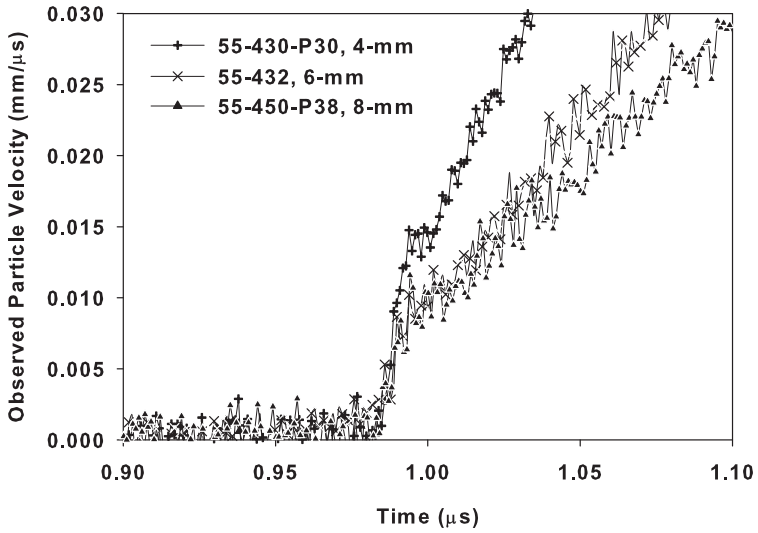

Figure 1. Elastic precursor amplitude observed in VISAR signals of transmission experiments having 3 different Be target thicknesses. Particle velocities for experiment 55-450-P38 have been scaled to correct for the influence of the LiF analyzer window employed in this experiment.

The raw VISAR data from which the HEL is calculated for 3 of the transmission geometry experiments having nominal Be target thicknesses of 4 mm (55-430-P30), 6 mm (55-432), and 8 mm (55-450-P38) is presented in Figure 1. While VISAR data was collected at times both earlier and later than what is shown in Figure 1, only the timespan around the elastic precursor wave is shown. The observed particle velocity data of experiment 55-432 has been scaled to reflect the fact that the VISAR data was obtained looking through a LiF window, while for the others, VISAR data was collected from direct observation of the free surface of the Be target. Also, the timescales for all VISAR traces have been artificially shifted to bring the foot of the rise in particle velocity associated with the elastic precursor into coincidence.

The key feature to note in Figure 1, is that as target thickness is increased between 4 and 8 mm the amplitude of the precursor wave observed in the VISAR traces decreases, with most of the decrease occurring between 4 and 6 mm and little additional decrease in amplitude between 6 and 8 mm target thickness. Expressed another way, the magnitude of the HEL calculated from the VISAR data, a measure of the dynamic yield strength of the Be, decreases with increasing elastic precursor propagation distance through the Be. This is further illustrated by the data presented in Figure 2 which shows graphically all of the HEL data from transmission geometry shots in Table 1 plotted against Be target thickness. The black curve shown in the figure is a simple least squares logarithmic fit to the black data points plotted in the figure. The functional form of the fit is $y = y_0 + a[ln((x - x_0)/x_1)]$ where y_0 = 0.04 GPa, a = -0.0506 GPa, x_0 = 2.556 mm and x_1 = 12.54 mm. The red data points, derived from experiments 55-429 and 55-466, were excluded from the fit since we calculated and plotted two values of the HEL for these experiments. In both cases, the shock velocity computed using the measured target impact time from PZT pins, the elastic precursor wave breakout time at the rear surface of the target from VISAR, and the known physical thickness of the sample provided shock velocities lower than the longitudinal sound speed (c_L) measured pre-shot. Since the elastic precursor wave speed should be c_L we believe there is an intermittent timing error for these two experiments that lead to the lower than expected elastic precursor velocities. For the sake of completeness, the values of the

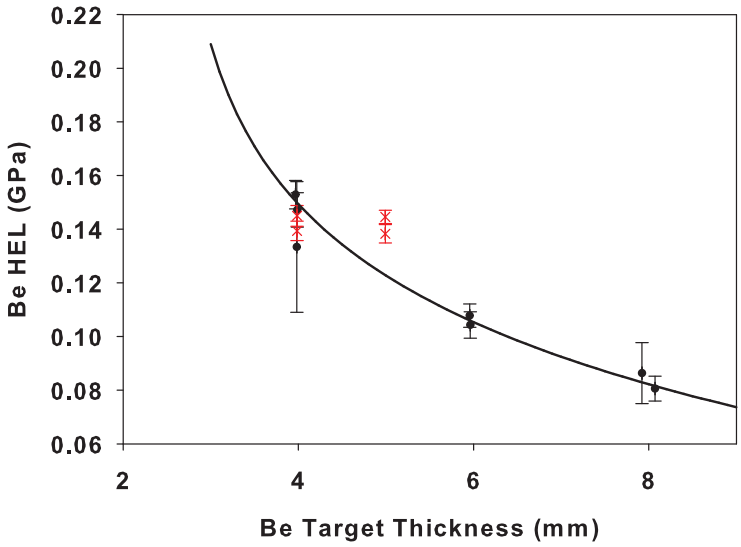

Figure 2. Hugoniot elastic limit (HEL) calculated for each transmission experiment in Table 1 as a function of the VHP S200-F Be target thickness.

HEL computed using both velocities are still presented in the figure for each experiment.

We believe the decay in elastic precursor amplitude with Be target thickness is observable in Be due to the sluggish kinetics associated with the transition in material response from initial elastic behavior to a mix of elastic and plastic deformation. Unlike metals having either the body centered cubic (bcc) or face-centered cubic (fcc) crystal structure, for which there are a large number of active primary slip systems (12) for dislocation-mediated slip, hcp metals such as Be have a limited number (3) of primary slip systems and only an additional 3 secondary slip systems.[4] As a result, greater propagation distance is required of the elastic precursor wave in Be before a stable two wave structure consisting of an elastic precursor wave running out a head of a trailing plastic wave is achieved through dislocation-mediated slip mechanisms. In the case of Be, this transition persists to a target thickness of at least 8 mm. We are precluded from performing transmission geometry experiments on Be target thicknesses greater than 8 mm on the 41 mm bore gun where this work was performed due to the potential intrusion of edge release waves at the center of the target where VISAR observations are made for target thicknesses greater than 8 mm.

It has been proposed by others [5] that the limitations of dislocation-mediated slip in hcp metals opens the door to the other slip mechanisms such as mechanical twinning to help expedite the transition from the initial elastic material response to a mix of elastic and plastic behavior. The crystallographic re-orientation introduced through twinning may help to more favorably align inactive slip systems relative to the deformation axis for dislocation-mediated slip in addition to simply providing a second mechanism of plastic deformation.

A further illustration of the sluggish kinetics associated with the decay of elastic precursor amplitude with propagation distance in Be is illustrated by the VISAR data from a plate impact experiment in reverse geometry (55-476). The shot parameters for the experiment are documented in Table 1 and the VISAR data obtained is presented Figure 3. Reverse geometry, in which the material being interrogated is thrown at an analyzer window, offers the possibility of observing the earliest stages of the precursor decay process since wave evolution is observed beginning at the impact surface rather than after waves(s) have propagated through the target

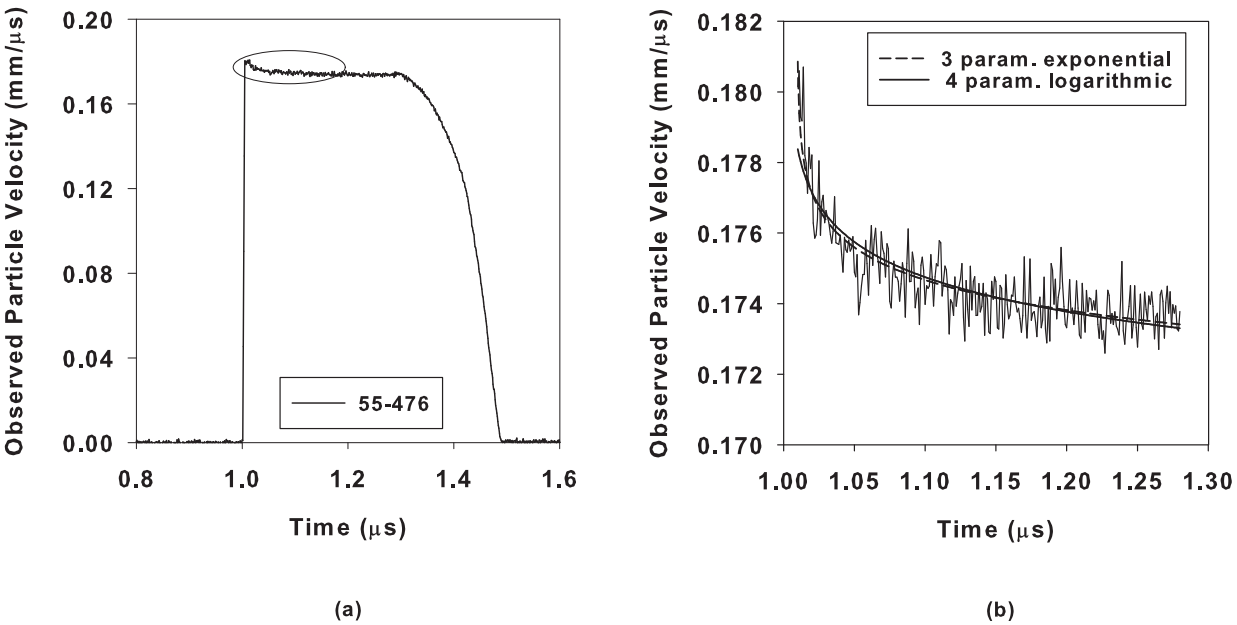

Figure 3. VISAR wave profile (3a) obtained in reverse geometry experiment 55-476 and an expanded view of the region enclosed in an oval in 3a showing the temporal relaxation of the initial elastic response of the VHP S-200F Be observed in the Z-Sapphire analyzer window (3b).

thickness. This is illustrated by the relaxation in particle velocity displayed by the VISAR data in Figure 3a immediately following impact and prior to the time at which a steady state is achieved before release arrival; the region enclosed by an oval in Figure 3a. Figure 3b is an expansion of the region enclosed within the oval of Figure 3a. Initial attempts to fit the temporal evolution of the data in Figure 3b with either a 4-parameter logarithmic expression of the form used to fit the data in Figure 2 ($y = y_0 + b[ln((t - t_0)/\tau)]$); where y_0 = 0.1739 mm/μs, b = -0.0011 mm/μs, t_0 = 1.003 μs and τ = 0.179 μs or a 3-parameter exponential of the form: $y = y_0 + a[exp(t - t_0)]$ where y_0 = 0.1739 mm/μs, a = -0.0011 mm/μs and t_0 = 1.0096 μs are presented in the figure. Both functional forms fit the data rather well. The 3-parameter exponential fit provides little more than a fit to guide the eye since the argument of the exponential is not normalized to be dimensionless. At the time of this writing we did not have a corresponding 4-parameter exponential fit to the data. Furthermore, we have no fundamental physical basis favoring one functional form over the other. The 4-parameter logarithmic function does not fit the data as well as the 3-parameter exponential, but proper normalization of the argument of the logarithm has been applied. As such, the parameter, τ, does provide a time-constant for the decay of the elastic response of 0.179 μs which will be incorporated into future efforts to underpin models of the observed relaxation with underlying physical processes of dislocation dynamics and/or mechanical twin formation.

4. Summary

We have performed a successful series of transmission and reverse geometry plate impact experiments on VHP S-200F Be which have provided an opportunity to examine the process of elastic precursor decay with precursor propagation distance. Exponential and logarithmic

fits to the observed decay in HEL with target thickness provide at the very least a predictive capability of expectations for future experiments. In addition, the relaxation of the elastic response observed in the single reverse geometry experiment we have performed to date provided a time constant for the relaxation which will be a key feature incorporated in any efforts to model the relaxation behavior. Additional experiments are planned in both transmission and reverse geometry to provide HEL data for Be target thicknesses less than the 4 mm minimum thickness examined to date and to examine the influence of the initial crystallographic texture of the S200-F Be on the HEL relaxation in both transmission and reverse geometries.

4.1. Acknowledgments
This research was performed at Los Alamos National Security, LLC for the U. S. Dept. of Energy, National Nuclear Security Administration, under contract DE-AC52-06NA25936.

References

[1] Blumenthal, W R, Abeln, S P, Cannon, D D, Gray III, G T and Carpenter, R W, *Shock Compression of Condensed Matter - 1997, AIP Conference Proceedings 429*, **1**, 411–14, (1997)
[2] Marsh S P 1980 *LASL Shock Hugoniot Data* (Univ. of CA Press, CA)
[3] Adams, C D, Anderson, W W, Gray III, G T, Blumenthal, W R, Owens, C T, Freibert, F J, Montoya, J M and Contreras, P J, *Shock Compression of Condensed Matter - 2009, AIP Conference Proceedings 1195*, **1**, 509–12, (2009)
[4] Reed-Hill, R E, 1973 *Physical Metallurgy Principles* (D. Van Nostrand Co.)
[5] Brown, D W, Beyerlein, I J, Sisneros, T A, Clausen, B and Tome, C N, 2012 *Int. J Plastic.* **29** 120–35